NASA Technical Paper 2218

November 1983

Proposed Fast-Response Oxygen Monitoring and Control System for the Langley 8-Foot High-Temperature Tunnel

Jag J. Singh,
William T. Davis,
and Richard L. Puster

NASA

25th Anniversary
1958-1983

NASA
Technical
Paper
2218

1983

Proposed Fast-Response Oxygen Monitoring and Control System for the Langley 8-Foot High-Temperature Tunnel

Jag J. Singh,
William T. Davis,
and Richard L. Puster

Langley Research Center
Hampton, Virginia

NASA
National Aeronautics
and Space Administration

**Scientific and Technical
Information Branch**

1983

INTRODUCTION

Projected plans call for the modification of the Langley 8-Foot High-Temperature Tunnel (8-ft HTT) in order to provide a test medium suitable for hypersonic, air-breathing-engine studies (refs. 1 and 2). As presently configured, methane gas is burned in air under pressure and the products of combustion are expanded through an axisymmetric, conical contoured nozzle with an exit diameter of 8 ft to produce a nominal Mach 7 flow in the test section. However, because of the reduced oxygen content in the test medium, the facility is not currently suitable for air-breathing-propulsion testing. The proposed modification would increase the oxygen concentration of the air going into the combustor so as to provide the same oxygen concentration as normal air in the test medium.

The maintenance of equivalent air in the test section is very important for successful hypersonic-vehicle development studies. Too much oxygen may damage the engine, and too little oxygen will result in reduced impulse. Because of limited run time of the facility (as little as 20 sec for some conditions), a fast-response (Response time $\leq$ 1 percent of the tunnel run time) oxygen monitoring and control system is required.

The methane oxidation reaction in oxygen-enriched air can be written as follows:[1]

$$n(CH_4) + m(O_2) + \text{Air} \longrightarrow n(CO_2) + 2n(H_2O) + (m - 2n)(O_2) + \text{Air} + \text{Heat} \qquad (1)$$

Input channel — Output channel

To produce the highest temperature in the output channel, the amount of O_2 added to the input channel should be just sufficient to fully oxidize the CH_4 gas. However, to make the O_2 mole fraction in the output channel the same as in normal air - namely, 0.2095 - it will be necessary to add extra O_2 to the input channel (ref. 5).

From equation (1), it is easily seen that:

$m/n = 2.795$, if no H_2O is removed from the output channel.

$m/n = 2.265$, if all H_2O is removed from the output channel.

$m/n = 2.265 + 0.265(P_3/n)$, if only part of the H_2O is removed from the output channel, where P_3 is the partial pressure of H_2O vapor in the test gas.

---

[1]Actually, the combustion of methane in oxygen-enriched air is a much more complex process than that indicated by equation (1). Further details of this process can be found in references 3 and 4. However, equation (1) is adequate for the purpose of describing the requirements for an oxygen sensor in the present study.

This report describes the development and testing of a proposed fast-response oxygen monitoring and control system for use in the modified 8-ft HTT.

LIST OF SYMBOLS

$O^{=}$	doubly negatively charged oxygen ion
e^{-}	electron
A	mathematical constant, characteristic of the cell and its operating temperature
C(P)	cell constant, a function of the total pressure in the cell cavity
F	Faraday constant
P	total gas pressure in cell cavity
P_1	partial pressure of oxygen in the reference gas
P_2	partial pressure of oxygen in the test gas
P_3	partial pressure of H_2O vapor in the test gas
R	gas constant
T	absolute temperature
T_D	time constant

OXYGEN MONITORING SYSTEM

Oxygen Sensor Selection

We have investigated the applicability of electrochemical sensors (refs. 6 and 7) for measuring oxygen concentration in the test section of the 8-ft HTT. These sensors are ideally suited for high-temperature applications. The most frequently used electrochemical oxygen detectors are the solid-state ceramic oxide devices, such as ZrO_2 and TiO_2 sensors (refs. 8 and 9). The ZrO_2 device is based on the Nernst equation, which relates the oxygen partial pressures on its opposite sides with the voltage potential difference developed across them. The TiO_2 sensors, on the other hand, are based on the principle that the intrinsic resistivity of TiO_2 is a function of the oxygen concentration in the test gas. Of these two types, ZrO_2 sensors are faster and more dependable in transient combustion environments (refs. 10 to 14). The recommended operating temperature range for ZrO_2 sensors is 600°C to 850°C (refs. 8 and 9). The high operating temperature is necessary in order to produce the vacancies that effect the oxygen ion diffusion through the sensor disc.

Figure 1 illustrates the theory of operation of the ZrO_2 oxygen sensor. The sensor is made of a high-temperature, Y_2O_3-stabilized ZrO_2 ceramic electrolyte disc coated with porous platinum electrodes on both sides. The platinum electrodes are porous enough to permit ready diffusion of gases through them. Oxygen, or an oxygen-containing gas such as air, is supplied to one side of the disc and the test gas is

supplied to the other side. Oxygen molecules arriving at the heated electrode are dissociated and converted to doubly charged oxygen ions, with the platinum electrode providing the necessary electrons; that is,

$$O_2 \longrightarrow 2O^{=} - 4e^{-} \tag{2}$$

The $O^{=}$ ions combine with the vacancies and diffuse through the heated ceramic disc to the other side where they convert to neutral O_2 molecules, with the platinum electrode taking up the extra electrons; that is,

$$2O^{=} \longrightarrow O_2 + 4e^{-} \tag{3}$$

When the concentration of oxygen is different on the two sides of the disc, more oxygen ions migrate from the high-oxygen-concentration side to the low-oxygen-concentration side. This ion flow provides an electronic imbalance which results in a voltage difference between the two platinum electrodes. The voltage difference is a function of the disc temperature and the oxygen partial pressures on the two sides of the disc. The voltage difference is given by the Nernst equation (refs. 6, 7, and 10):

$$E = \frac{RT_2}{4F} \ln \frac{P_1}{P_2} - \frac{3RT_2}{8F}\left[\ln\left(\frac{T_2}{T_1}\right) + \left(\frac{T_1}{T_2} - 1\right)\right] \tag{4a}$$

where

- E voltage difference across the two sides
- R gas constant
- T_2 temperature of the test gas
- F Faraday constant
- P_1 partial pressure of oxygen in the reference gas
- P_2 partial pressure of oxygen in the test gas
- T_1 temperature of the reference gas

If the test gas is at the same total pressure and temperature as the reference gas, this equation reduces to the following form:

$$E = \frac{RT}{4F} \ln \frac{P_1}{P_2} \tag{4b}$$

However, in practice the temperature and pressure are usually not exactly equal on the two sides of the sensor. Furthermore, the sensor matrix has impurities and

imperfections which also preclude direct use of equation (4b). A more practical relationship between the sensor output and the oxygen partial pressures on the two sides is given by the following equation:

$$E = AT \ln\left(\frac{P_1}{P_2}\right) + C(P) \tag{4c}$$

where

A mathematical constant

T ZrO_2 disc temperature

C(P) cell constant (determined by calibration with known gas mixtures at known pressures)

Because of the extreme sensitivity of the Nernst voltage to the ZrO_2 disc temperature, it is necessary to use a feedback loop - based on a thermocouple signal - to maintain the sensor temperature at a constant, high level of 843°C. A NiCr/NiAl thermocouple is used to monitor the temperature of the ZrO_2 sensor. An error signal, generated by comparing the thermocouple signal with a predetermined set point, is then used to maintain the sensor at 843°C.

Oxygen Sensor Calibration

Initially the ZrO_2 oxygen sensor was calibrated using various mixtures of $N_2 + O_2$ at room temperature. Figure 2 shows a schematic diagram of the experimental system used to develop the calibration graphs illustrated in figure 3. Figure 4(a) shows how the sensor output varies with the total pressure in the sensor cavity. The increase in the sensor output with increasing pressure reflects the effects of increasing oxygen partial pressure as well as slight changes in the cell constant C(P). Figure 4(b) shows how C(P) changes with the total cell cavity pressure. It is apparent that the predominant cause of increasing sensor output with increasing cavity pressure is the oxygen partial pressure increase. Figure 5 shows the response time of the oxygen sensor. From these figures, it is evident that (1) the sensor output is nearly linearly dependent on the oxygen concentration in the range of 20.95 ± 3.0 percent oxygen, (2) the cell constant C(P) is essentially independent of the total pressure in the pressure range investigated, and (3) the mean sensor response time defined by the time constant T_D is less than 1 sec. The experimental system was then modified to include the hydrocarbon combustion products in the test gas stream. Figure 6 shows the modified experimental system which introduced oxygen after the combustion process. A cold-water trap was introduced in the test circuit to ensure that the liquid-phase H_2O vapors[2] in the CH_4-O_2-air combustion products did not enter the oxygen sensor cavity. It also helps to more closely approximate the expansion of combustion gases into the wind tunnel test section, as indicated

---

[2]The gas phase water vapor does not affect the operation of the sensor. However, liquid phase water vapor can cause thermal shock. Keeping the test gas transport line hot can eliminate this problem.

later. The sensor output was studied as a function of variable oxygen inflow rates. Again, the sensor output was observed to vary linearly with the oxygen concentration in the range of 20.9 ± 3.0 percent oxygen and the cell response time was ≤1 sec.

Finally, the experimental system was modified so that a controlled amount of oxygen gas was introduced in the air prior to methane combustion, as would be the case in the combustor of the wind tunnel. Figure 7 shows the schematic diagram of the new system. Coverage of the same oxygen concentration range as was used to obtain the calibration graphs shown in figure 3 necessitated a flame sustenance well beyond a ratio of O_2 flow rate to CH_4 flow rate of 2.0. A new type of burner, illustrated in figure 8, was designed and constructed after it was found that the straight-stem burner could not sustain a flame beyond a ratio of O_2 flow rate to CH_4 flow rate of approximately 1.7. This new burner sustained the flame well beyond the design ratio of 2.0. Typical results obtained with this burner are summarized in table I. All subsequent tests were conducted with this burner.

After checking the burner operation for ratios of O_2 flow rate to CH_4 flow rate in the range of 0 to 2.5, the O_2-to-CH_4 flow-rate ratio was adjusted to produce the same oxygen sensor output as obtained with the room air. The combustion system was allowed to run for about 1 hour and its output was recorded on a strip chart recorder. The output stayed reasonably constant at -20.75 ± 0.16 mV as shown in figure 9.

In order to verify that the oxygen concentration of the products of the CH_4-O_2-air combustion which produced oxygen sensor output equal to that for air was indeed the same as in the room air, samples of room air and the exhaust gas were analyzed using a gas chromotograph. The results are summarized in table II. The oxygen concentration in the exhaust gas is equal to that in the reference air, confirming the reliability of operation of the oxygen monitoring system.

Sensor Response Time

As indicated previously, the oxygen-monitoring-system response time for the sudden switch of ambient-temperature $N_2 + O_2$ mixture to air was less than 1 sec. Although this may be adequate for some applications, it is still too large for the present application, wherein the total available experimental time is ≈1 minute. It would be highly desirable if the sensor response time could be reduced to 0.1 to 0.2 sec. The intrinsic ZrO_2 sensor response time is reportedly of the order of a few tens of milliseconds (refs. 8 and 9) and is thus not a determining factor in the overall sensor assembly response time. The following factors control the ZrO_2 sensor response time:

1. Temperature sensitivity of the Nernst voltage across the ZrO_2 sensor

2. Time to flush out gas from the sensor cavity

In order to avoid the increase of the sensor response time caused by the cooling effect of the room-temperature test gas arriving at the sensor disc, the test gas was preheated to about the same temperature as the sensor disc (≈843°C). The sensor cavity was reduced in volume to less than 1 cm^3. Also, the test gas was introduced from the top of the cylindrical cavity and allowed to escape through a 0.5-mm-wide circumferential gap about 0.5 mm above the detector mount top. This arrangement allowed quick flushing of the gases from the detector cavity as well as exposure of the entire detector face to the test gas. Figure 10 shows the test gas preheating

arrangement. Figure 11 shows a schematic diagram of the modified sensor cavity. A complete oxygen sensor assembly - including the burner, heated test gas, transport tubings, and associated readout components - is shown in figure 12.

Figure 13 shows typical sensor-response-time results for various $N_2 + O_2$ mixture to air changes obtained by using the modified experimental arrangement. The $N_2 + O_2$ to air changes were effected almost instantaneously by using three-way electric solenoid valves. Therefore, the observed response times approached the true response time of the O_2 detection element. The experimentally measured overall system response times were of the order of 0.2 sec.

OXYGEN CONTROL SYSTEM

Having developed an oxygen monitoring system with a response time of the order of 0.2 sec, attention was directed towards developing a circuit for controlling the oxygen concentration of the reacted test gases. Figure 14 shows a schematic diagram of the control circuit developed for this purpose. A voltage signal equal to the sensor output for normal air - obtained just prior to the beginning of the tunnel run - is applied to one side of the summing amplifier and the test gas signal - obtained during the tunnel run - is applied to the other side. The difference between these two signals is amplified by a factor of 100. The resulting error signal - after appropriate attenuation and with appropriate polarity change - is made available to the oxygen control system. The error signal application can be delayed by a period equal to the settling time for the initial oxygen spray rate setting. Provisions have been made for continuous visual display of the test gas signal output as well as the error signal, indicating how far off the normal air the test gas composition is. If the error signal reaches the 25-percent mark, an alarm is sounded and an emergency tunnel shutdown signal is provided. The oxygen-limit alarm circuit is shown in figure 15.

The control system has been tested in the laboratory using simulated electrical signals corresponding to various $N_2 + O_2$ mixtures and CH_4-O_2-air combustion product gases as the test media, and it has been found to perform according to specifications.

INTEGRATION OF OXYGEN MONITORING AND CONTROL SYSTEMS

The oxygen monitoring and control circuits have been integrated to provide a compact monitoring and control system for the Langley 8-Foot High-Temperature Tunnel. Figure 16 shows a schematic diagram of the overall system assembly. An Apple II microcomputer provides running information about the various critical flow rates, sensor cavity pressure, sensor temperature, sensor voltage output, and error signal.

The integrated monitoring and control system has been successfully tested in the laboratory for various $N_2 + O_2$ mixtures and CH_4-O_2-air combustion product gases. The CH_4-O_2-air combustion product laboratory results should be directly applicable to the wind tunnel test section conditions. The use of the cold-water trap in the laboratory tests approximates - in an essential way - the changes in the reacted-gas composition that occur when it expands into the wind tunnel test section (ref. 15).

CONCLUDING REMARKS

A system for monitoring and controlling the oxygen concentration in CH_4-O_2-air combustion product gases in the Langley 8-Foot High-Temperature Tunnel has been designed and tested in the laboratory. The oxygen sensor is Y_2O_3-stabilized ZrO_2 ceramic disc maintained at 843°C. The overall system response time has been reduced to about 0.2 sec (≤1 percent tunnel run time). When the test gas oxygen concentration differs from the normal air concentration by 25 percent or more, an audio alarm is sounded and an emergency tunnel shutdown signal is provided. The laboratory tests of the prototype system have been quite successful.

Langley Research Center
National Aeronautics and Space Administration
Hampton, VA 23665
September 23, 1983

REFERENCES

1. Henry, J. R.; and McLellan, C. H.: Air-Breathing Launch Vehicle for Earth-Orbit Shuttle - New Technology and Development Approach. J. Aircr., vol. 8, no. 5, May 1971, pp. 381-387.

2. Hearth, Donald P.; and Preyss, Albert E.: Hypersonic Technology - Approach to an Expanded Program. Astronaut. & Aeronaut., vol. 14, no. 12, Dec. 1976, pp. 20-37.

3. Combustor Modelling. AGARD-CP-275, Feb. 1980.

4. Palmer, Howard B.; and Beér, J. M., eds.: Combustion Technology: Some Modern Developments. Academic Press, Inc., 1974.

5. Croom, Bobby H.; and Leyhe, Edward W.: Thermodynamic, Transport, and Flow Properties for the Products of Methane Burned in Oxygen-Enriched Air. NASA SP-3035, 1966.

6. Daniels, Farrington; and Alberty, Robert A.: Physical Chemistry, Third ed. John Wiley & Sons, Inc., c.1966.

7. Friend, J. Newton: A Textbook of Physical Chemistry, Abridged and Revised (Second) ed. Charles Griffin & Co., Ltd., 1948.

8. Grubar, H. U.; and Wiedenmann, H. M.: Three Years Field Experience With Lambda-Sensors in Automotive Control Systems. [Preprint] 800017, Soc. Automot. Eng., Inc., Feb. 1980.

9. Bobeck, Richard F.: Electrochemical Sensors for Oxygen Analysis. Chem. Eng., vol. 87, no. 14, July 14, 1980, pp. 113-117.

10. Shulman, M. A.; Hamburg, D. R.: Non-Ideal Properties of ZrO_2 and TiO_2 Exhaust Gas Oxygen Sensors. [Preprint] 800018, Soc. Automot. Eng., Inc., Feb. 1980.

11. Harmann, E.; Mangu, H.; and Steinke, L.: Lambda-Sensor With Y_2O_3-Stabilized ZrO_2-Ceramic for Application in Automotive Emission Control Systems. [Preprint] 770401, Soc. Automot. Eng., Inc., Feb. 1977.

12. Hetrick, Robert E.; Fate, W. A.; and Vassell, W. C.: Oxygen Sensing by Electrochemical Pumping. Appl. Phys. Lett., vol. 38, no. 5, Mar. 1981, pp. 390-392.

13. Hetrick, Robert E.; and Vassell, W. C.: Transistor Action Using ZrO_2-Electrochemical Cells. J. Electrochem. Soc., vol. 128, no. 12, Dec. 1981, pp. 2529-2536.

14. Young, C. T.: Experimental Analysis of ZrO_2 Oxygen Sensor Transient Switching Behavior. [Preprint] 810380, Soc. Automot. Eng., Inc., Feb. 1981.

15. Klich, George F.: Thermodynamic, Transport, and Flow Properties of Gaseous Products Resulting From Combustion of Methane-Air-Oxygen Mixtures. NASA TN D-8153, 1976.

TABLE I.- OXYGEN SENSOR OUTPUT AS A FUNCTION OF RATIO OF O_2 FLOW RATE TO CH_4 FLOW RATE IN THE CH_4-O_2-AIR COMBUSTION PROCESS[a]

[Ref. gas (air) flow rate of 1000 cm^3/min at 760 torr]

CH_4 flow rate, cm^3/min (b)	O_2 flow rate, cm^3/min (c)	$\frac{O_2 \text{ flow rate}}{CH_4 \text{ flow rate}}$, m/n	Air flow rate, cm^3/min	Test gas pressure in cell cavity, P, torr	Cell output, mV	
0	0	0	1700	755.8	-20.75	
0	0	0	1700	749.5	-20.56	≡Air
207.0	119.3	0.58 ± 0.03	1500	748.9	+60.67	
207.0	164.9	0.80 ± 0.04	1500	749.1	+13.65	
207.0	199.8	0.97 ± 0.04	1500	749.1	+ 4.85	
207.0	239.6	1.16 ± 0.04	1500	749.1	- 1.65	
207.0	279.4	1.35 ± 0.05	1500	749.2	- 6.31	
207.0	303.6	1.47 ± 0.05	1500	749.3	- 8.91	
207.0	336.6	1.63 ± 0.05	1500	749.3	-11.70	
207.0	375.4	1.81 ± 0.05	1500	749.3	-14.40	
207.0	400.6	1.94 ± 0.06	1500	749.3	-16.04	
207.0	438.4	2.12 ± 0.06	1500	749.4	-18.03	
207.0	480.2	2.32 ± 0.06	1500	749.4	-20.00	
207.0	488.5	[d]2.36 ± 0.06	1500	749.5	-20.56	≡Air
207.0	499.6	2.41 ± 0.06	1500	749.5	-20.75	
207.0	509.3	2.46 ± 0.07	1500	749.5	-21.30	
207.0	548.1	2.65 ± 0.07	1500	749.5	-22.85	
207.0	584.9	2.83 ± 0.07	1500	749.6	-24.15	
207.0	480.2	2.32 ± 0.06	1500	749.4	-20.00	
193.2	480.2	2.49 ± 0.07	1500	749.7	-21.20	
179.4	480.2	2.68 ± 0.08	1500	750.0	-22.40	
162.2	480.2	2.96 ± 0.09	1500	750.3	-23.80	

[a]Of the exhaust gases, 1700 cm^3/min (air equivalent) were drawn through the O_2 sensor cell for all CH_4-O_2-air mixtures.

[b]Error value of ±3.5 cm^3/min.

[c]Error value of ±5.0 cm^3/min.

[d]The value which gave a signal equal to that for air is about 4 percent higher than the theoretical value of 2.27. This could be due to incomplete water removal. (For no water removed, the value is 2.8.) For example m/n = 2.36 suggests that the O_2 mole fraction (with complete H_2O removal) in the exhaust channel should be 21.82 percent. Gas chromatographic analysis of the exhaust gas indicates an O_2 fraction of 21.7 ± 0.6 percent. The diffusion column in the gas chromatograph automatically removes all H_2O vapor present in the exhaust gas sample before analysis. Equating the O_2 mole fraction at m/n = 2.36 to that in normal air suggests that approximately 17.9 percent of the H_2O produced in the combustion process is left in the exhaust stream.

TABLE II.- SUMMARY OF GAS COMPOSITION MEASUREMENTS

[Accuracy of CO_2 analysis is ±1.0 percent; accuracy of CO and CH_4 analyses is ±2.0 percent of the scale reading]

Molecular species	Reference (room) air	Test (exhaust) gas (a)
O_2, percent	20.6 ± 0.6	[b]21.7 ± 0.6
CO, ppm	0.21	30
CO_2, percent	0.03	[c]11.8 ± 0.6
CH_4, ppm	1.6	0.20

[a]The increase in CO_2 in the exhaust gas results from $CH_4 + 2O_2 \longrightarrow CO_2 + 2H_2O$. The residence of O_2 in the flame determines the amount of O_2 reacted with CH_4. The relatively low concentrations of CO and CH_4 in the exhaust gas indicate high combustion efficiency and adequate residence time. If the reaction were on the fuel-rich side of the stoichiometry, significant quantities of CO and CH_4 would be present in the reacted test gas. Obviously this is not the case in the present instance. (See refs. 3 and 4.)

[b]The diffusion column in the gas chromatograph automatically removes all H_2O vapor from the exhaust gas sample before analyzing it. Thus, the gas chromatographic value of 21.7 ± 0.6 percent should be compared with 21.82 percent expected for $m/n = 2.36$ with complete H_2O removal. (See footnote b of table I.)

[c]This value should be compared with the theoretical value of 11.6 percent, based on complete water removal from the exhaust channel. (For 17.9 percent H_2O left in the exhaust channel, CO_2 concentration is expected to be 11.2 percent. (See footnote b of table I.))

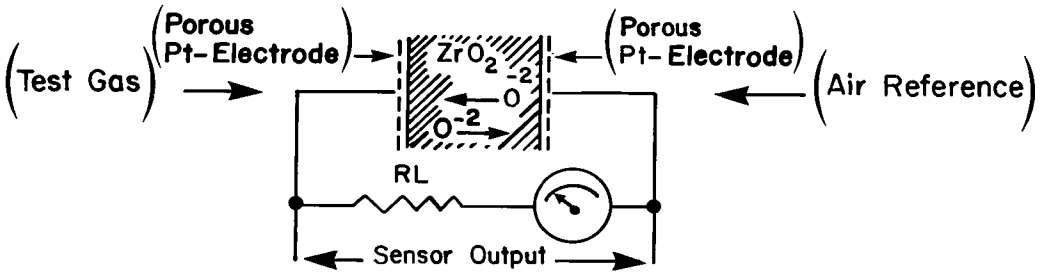

Figure 1.- Schematic illustration of principle of operation of ZrO_2 oxygen sensor.

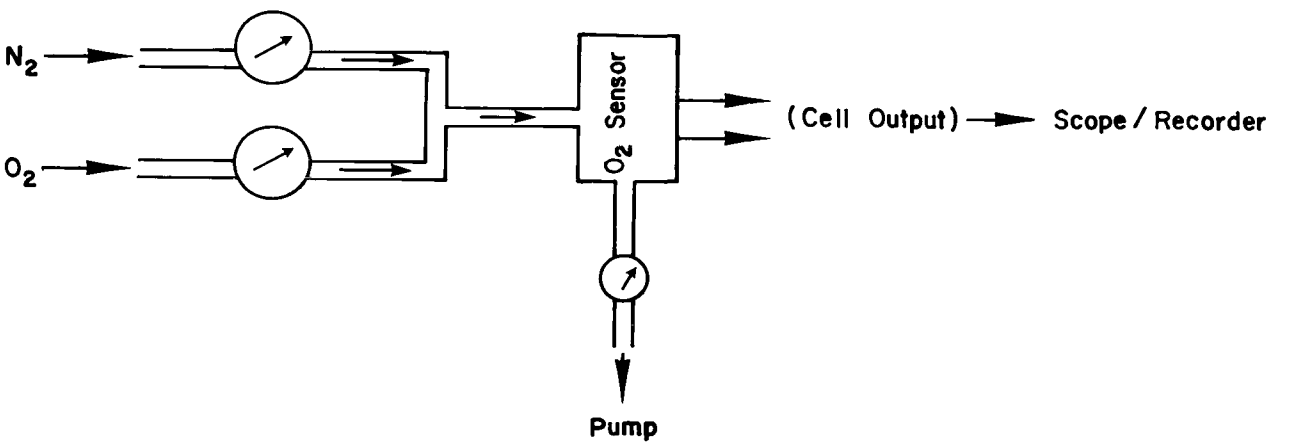

Figure 2.- Schematic illustration of oxygen sensor calibration system using $N_2 + O_2$ mixtures.

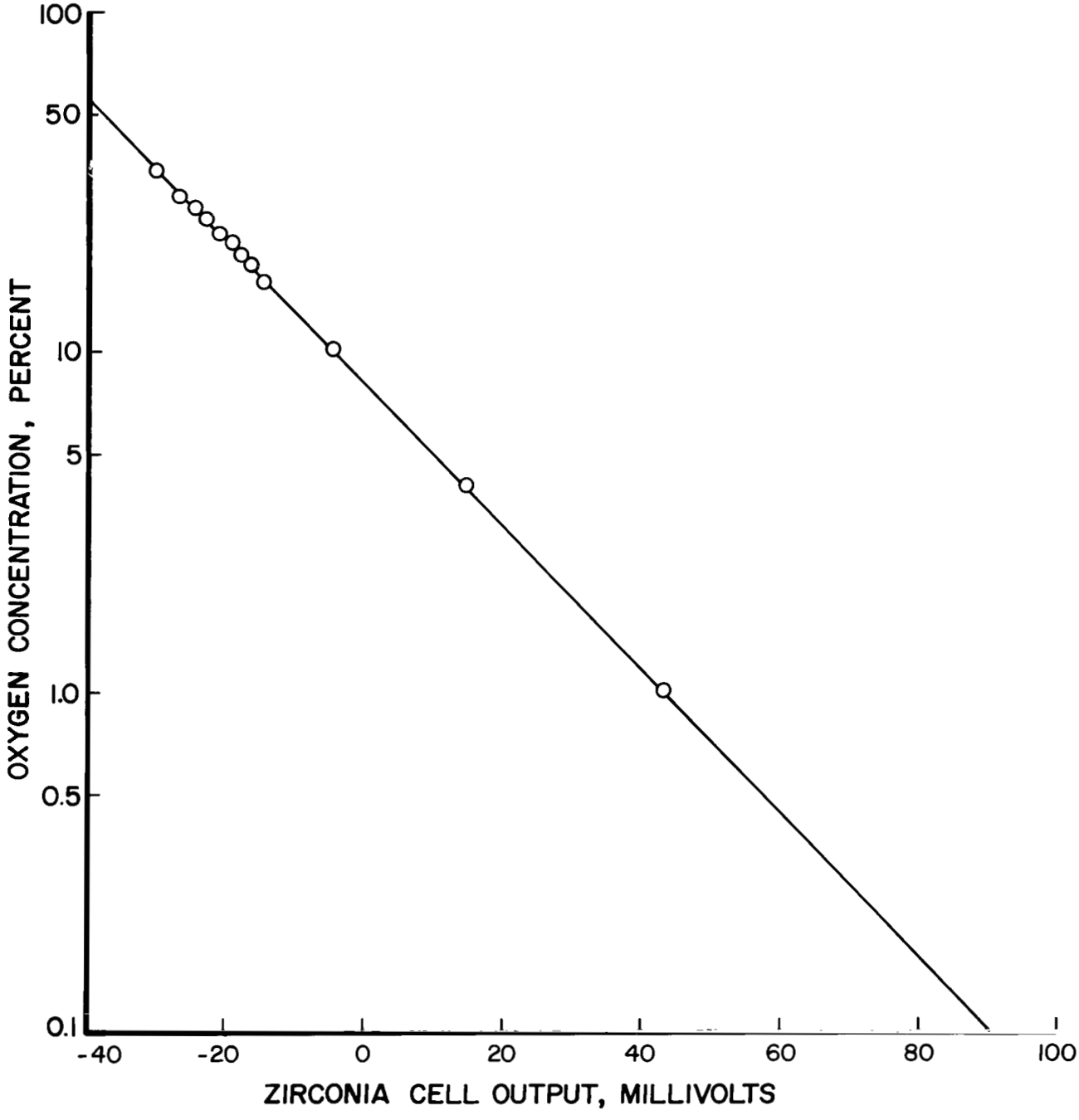

(a) Cell output as a function of oxygen concentration.

Figure 3.- Zirconium oxide oxygen sensor calibration.

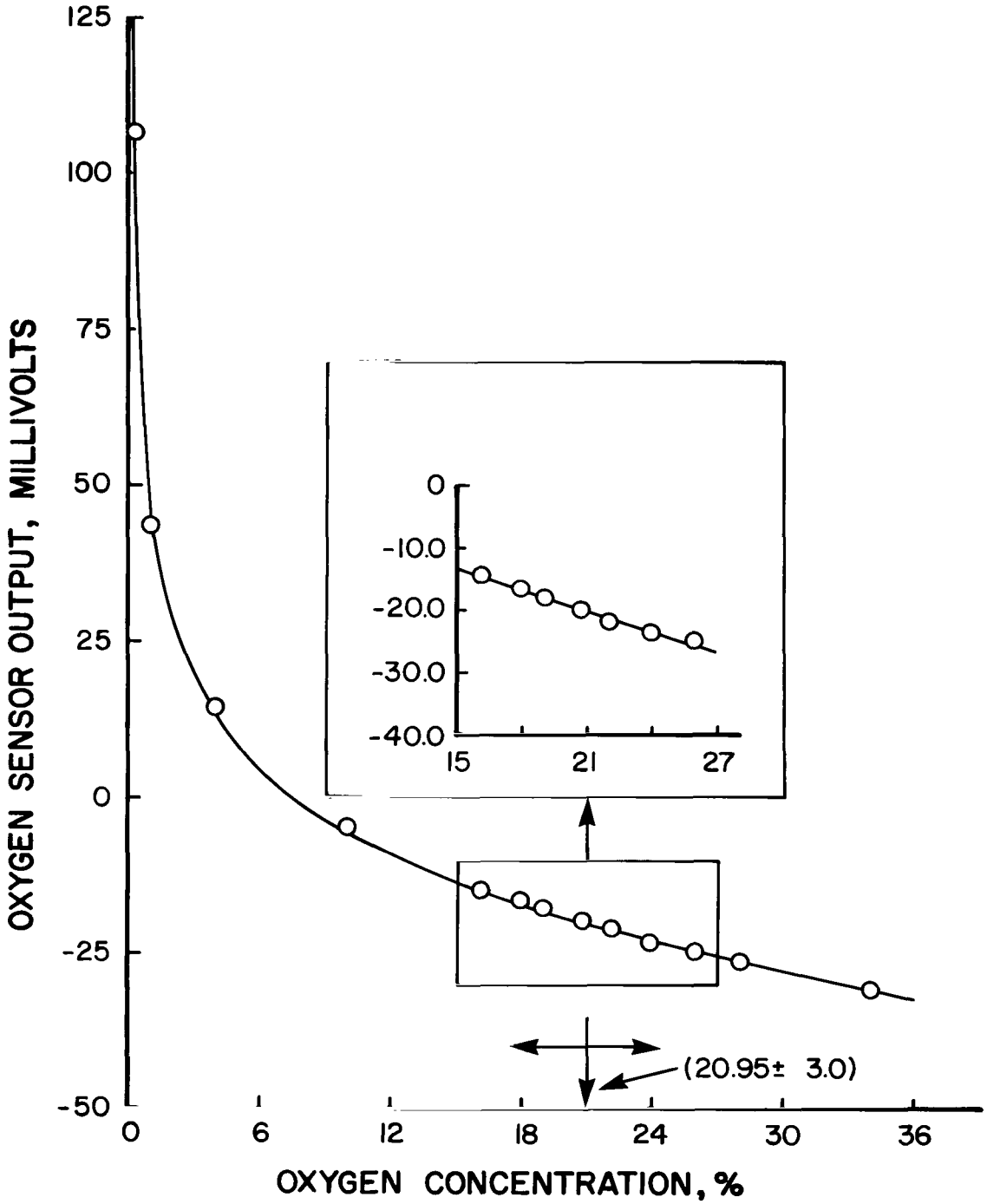

(b) Sensor output for range of oxygen concentrations.

Figure 3.- Concluded.

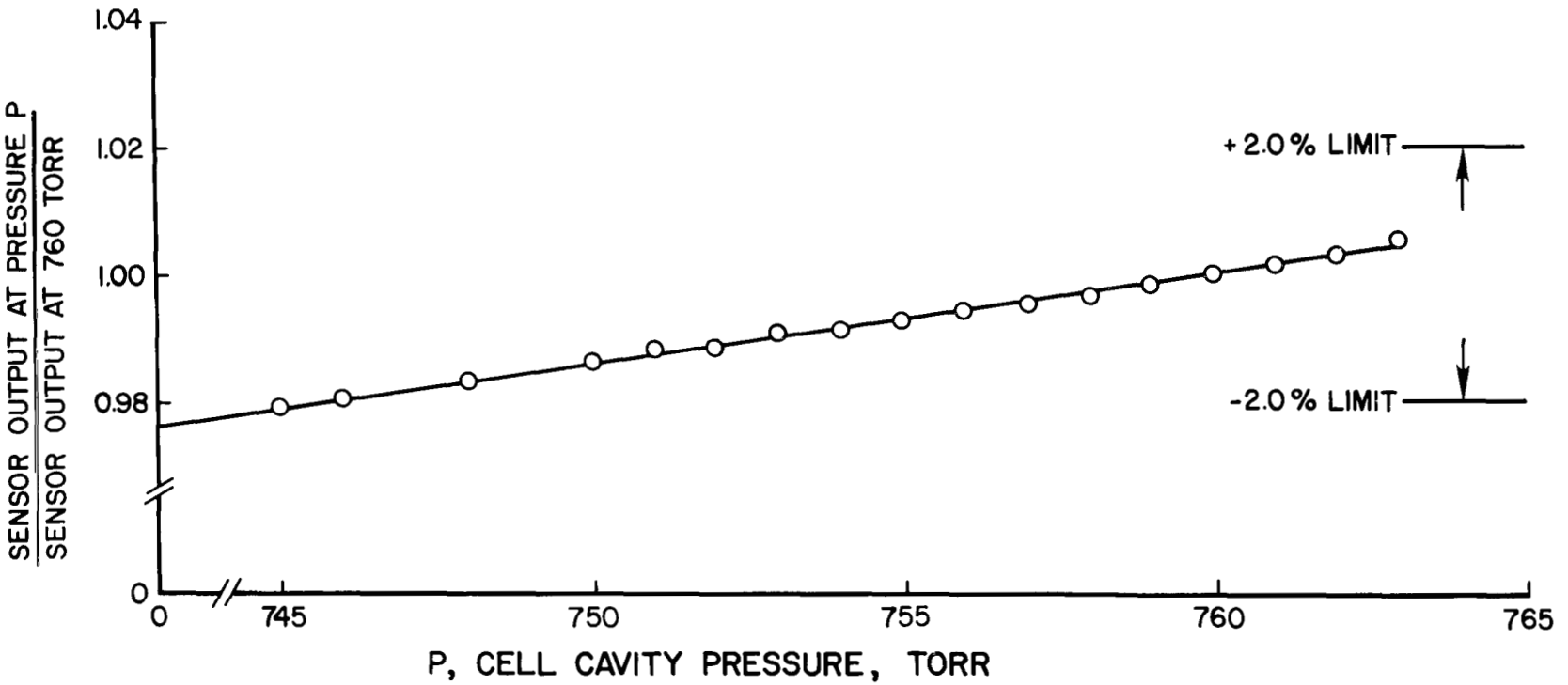

(a) Dependence of ZrO_2 sensor output for air on total pressure in the cell cavity.

Figure 4.- Relationship of ZrO_2 sensor output and cavity pressure.

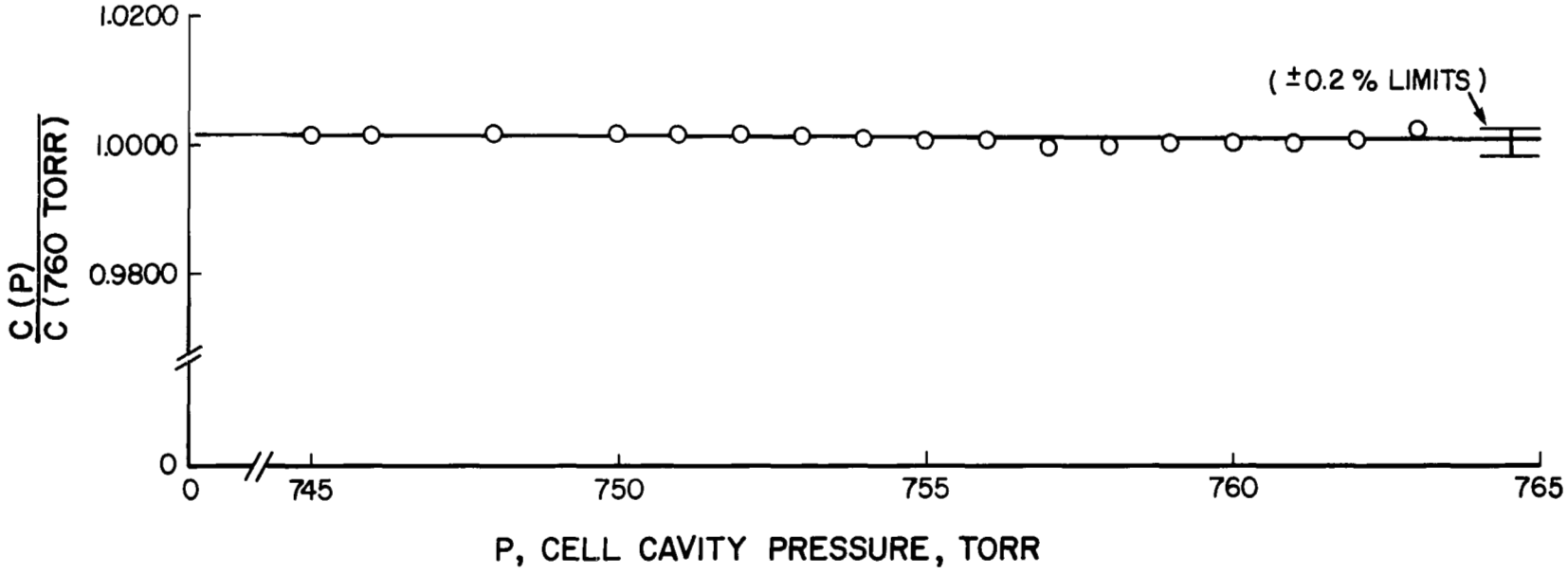

(b) Dependence of cell constant C(P) on total pressure in cell cavity.

Figure 4.- Concluded.

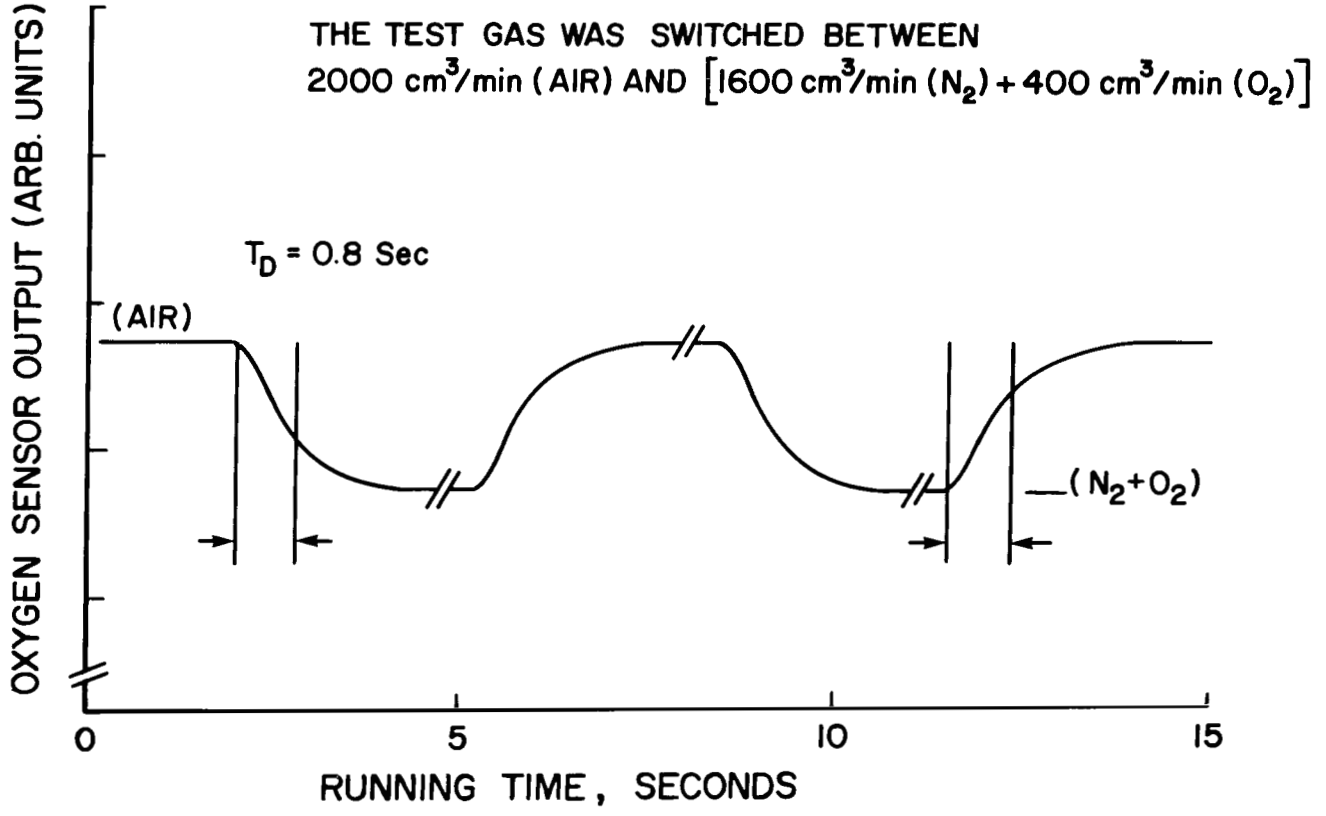

Figure 5.- Zirconium oxide oxygen sensor response time.

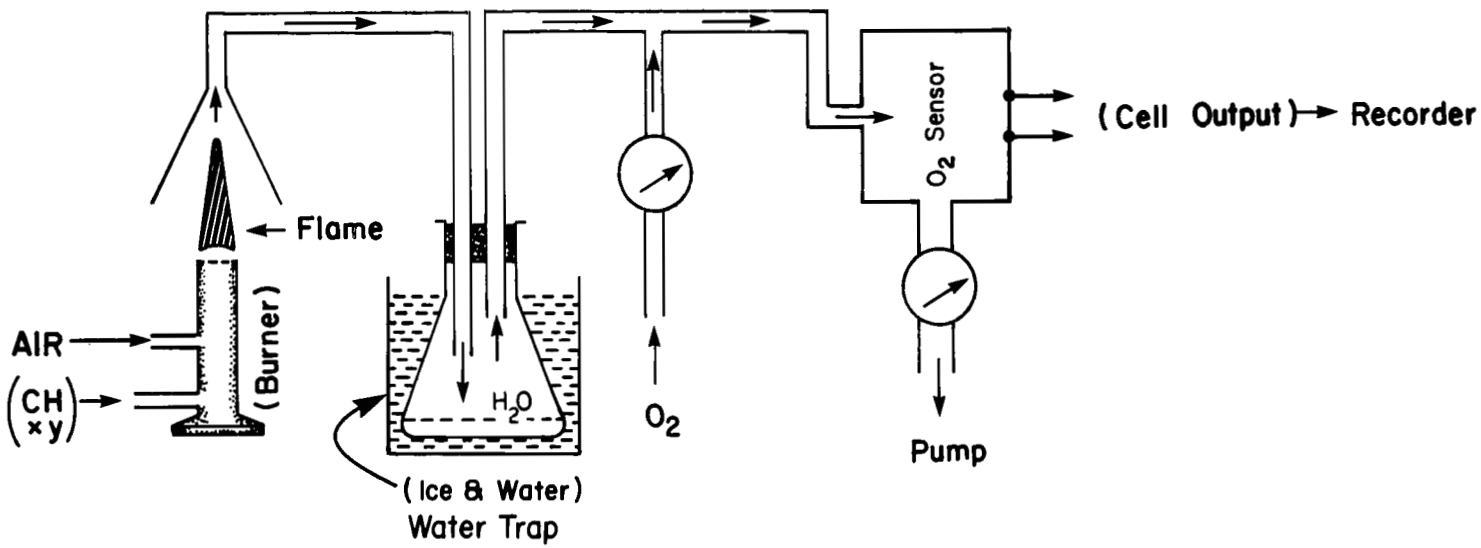

Figure 6.- Schematic diagram of ZrO_2 oxygen sensor calibration with CH_4 air combustion products mixed with O_2.

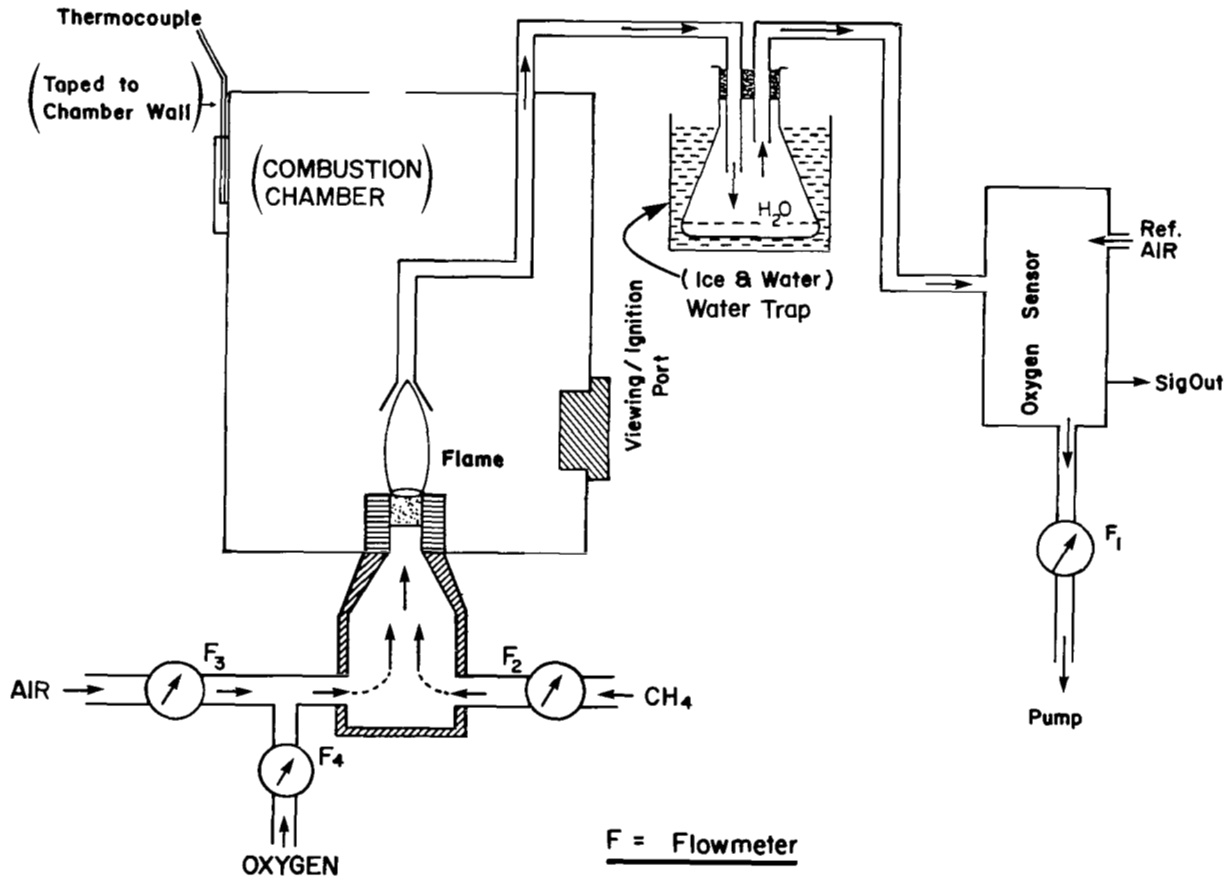

Figure 7.- Systematic diagram of experimental system for monitoring combustion exhaust gas composition using ZrO_2 oxygen sensor.

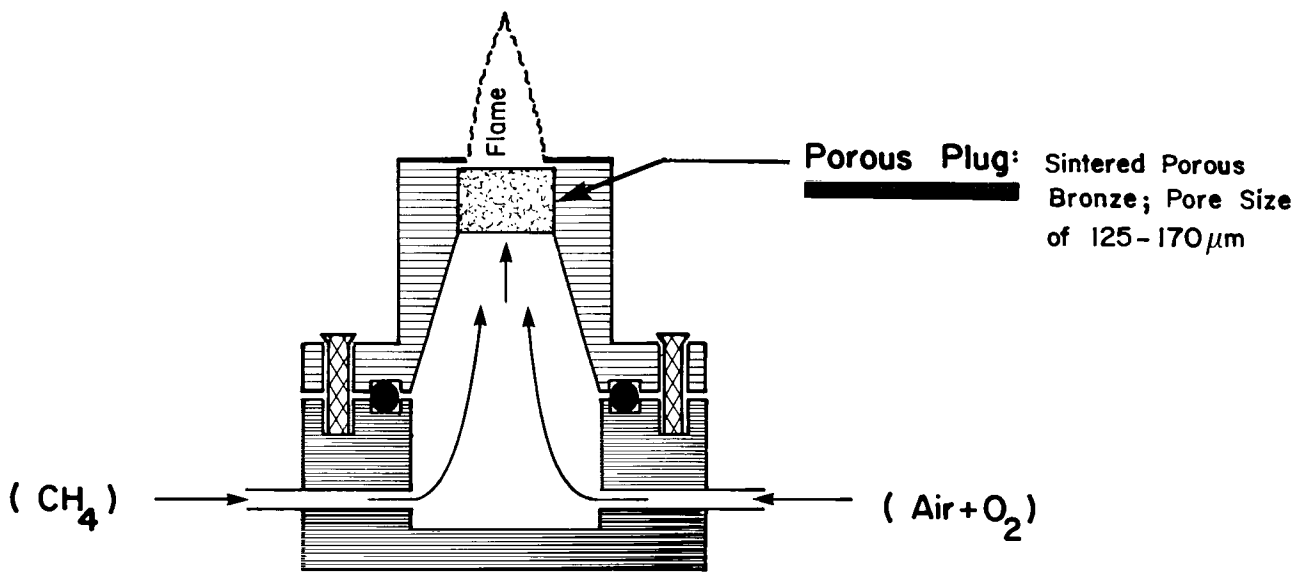

Figure 8.- Schematic diagram of modified methane burner.

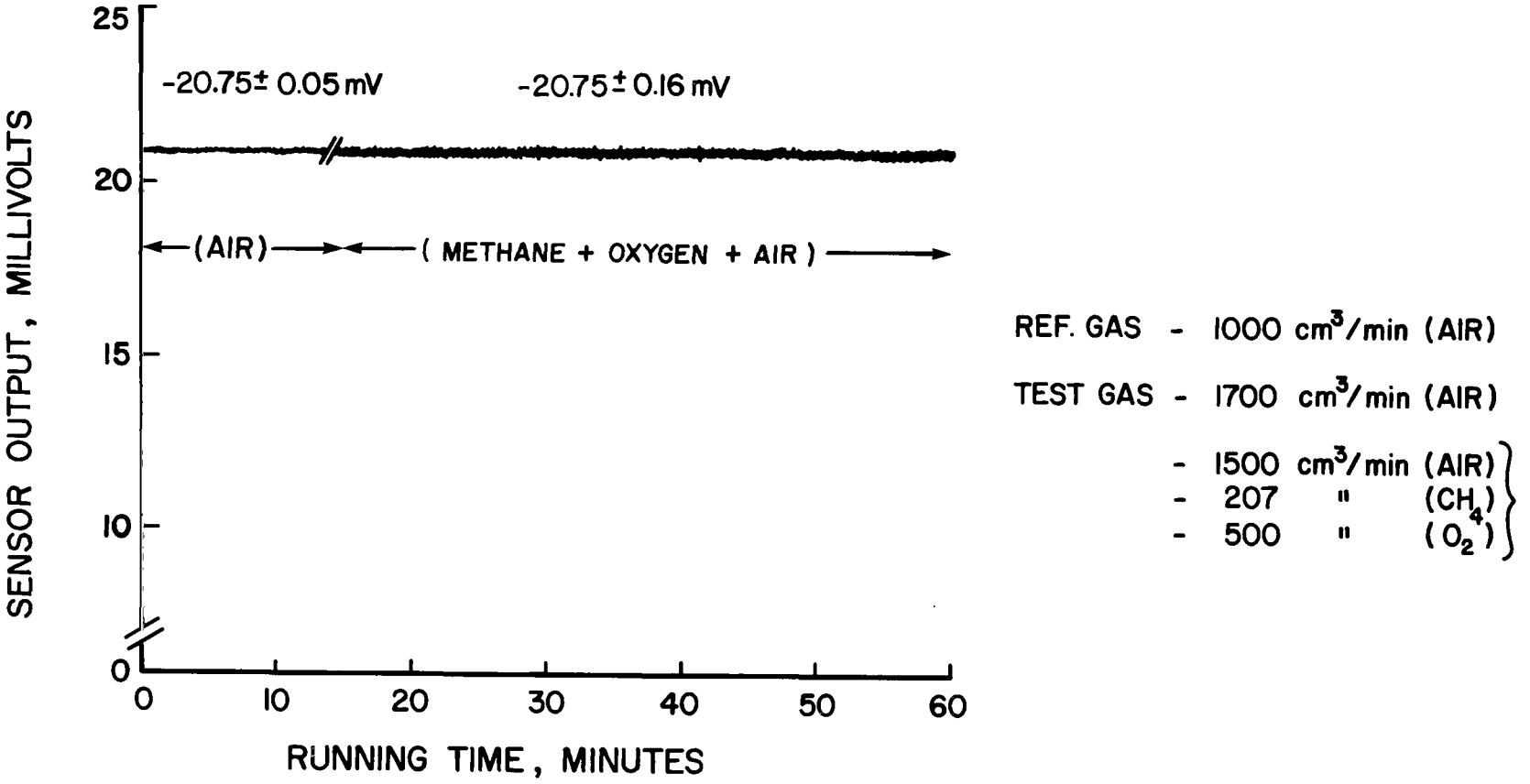

Figure 9.- Stability of ZrO_2 oxygen sensor output over an extended period.

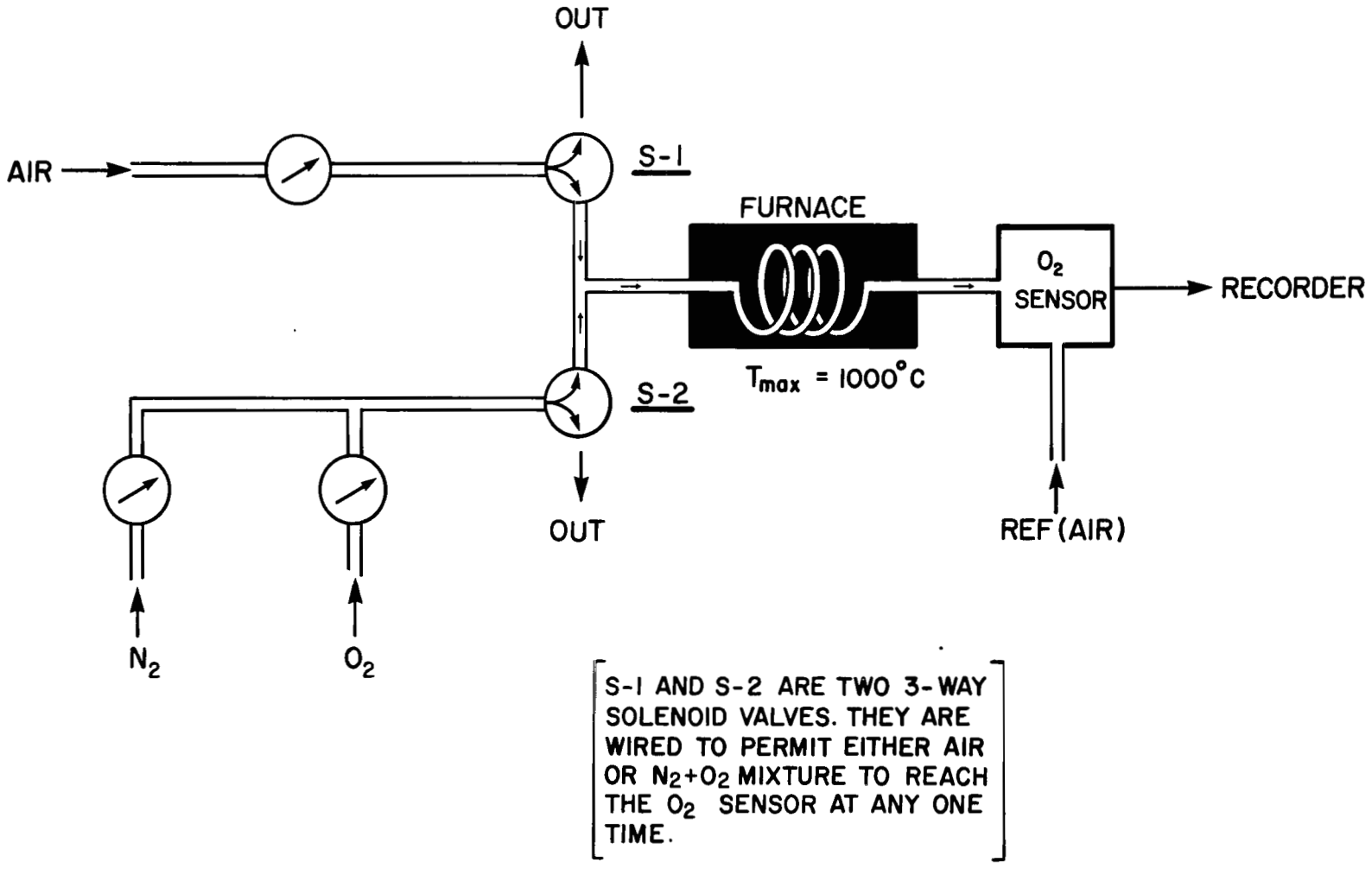

Figure 10.- Schematic diagram of experimental system for switching from air to N_2 + O_2 mixture and preheating the gases arriving at the O_2 sensor.

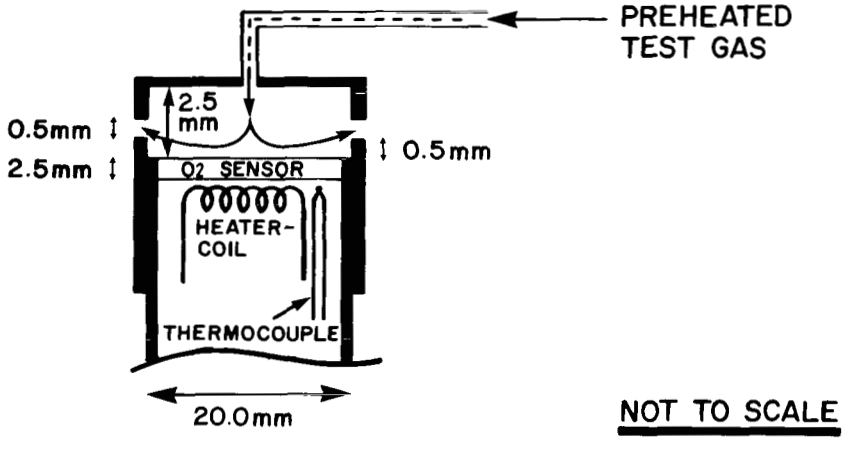

Figure 11.- Schematic diagram of the modified sensor cavity.

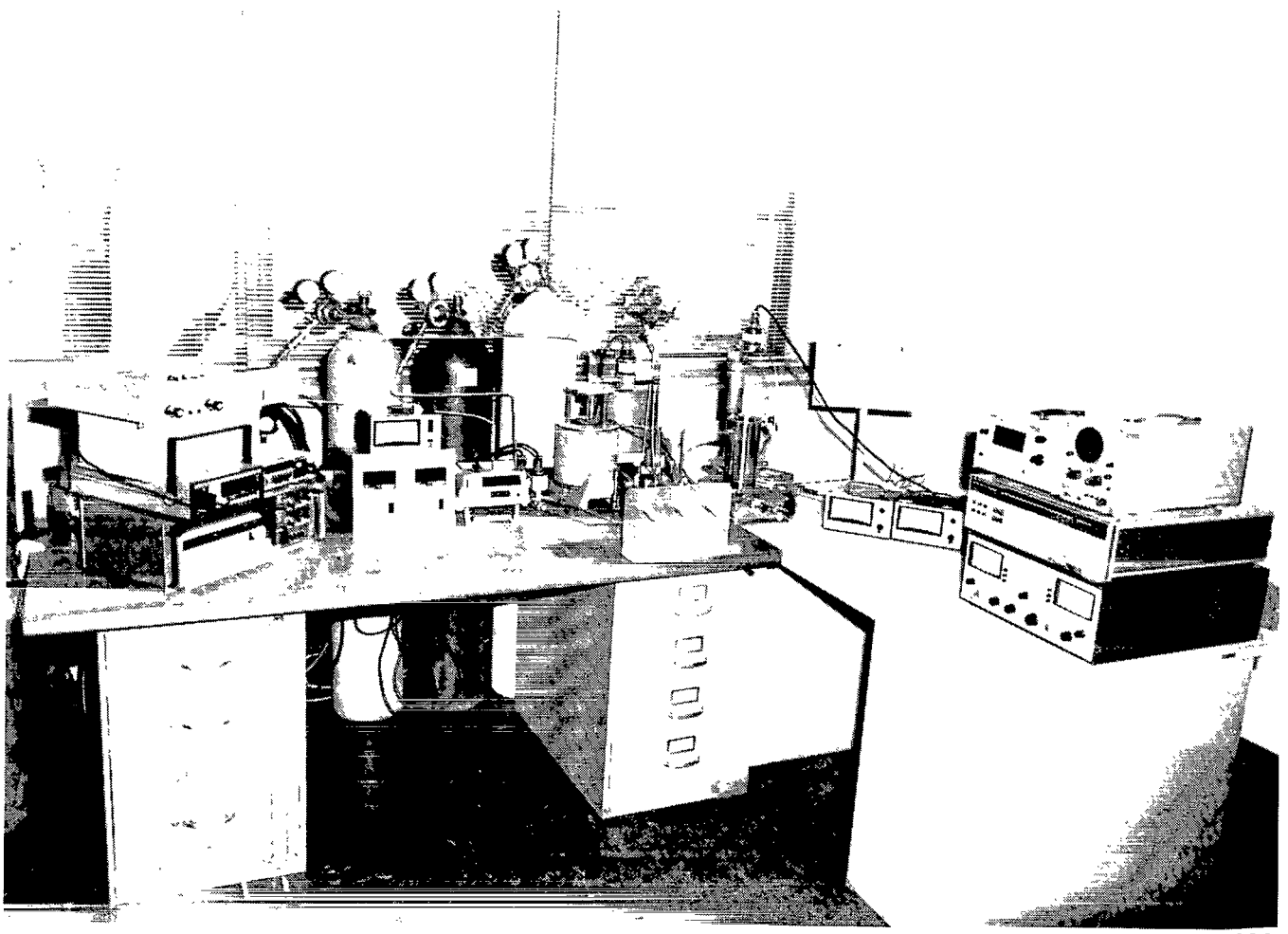

L-83-620

Figure 12.- Photograph of complete oxygen sensing system.

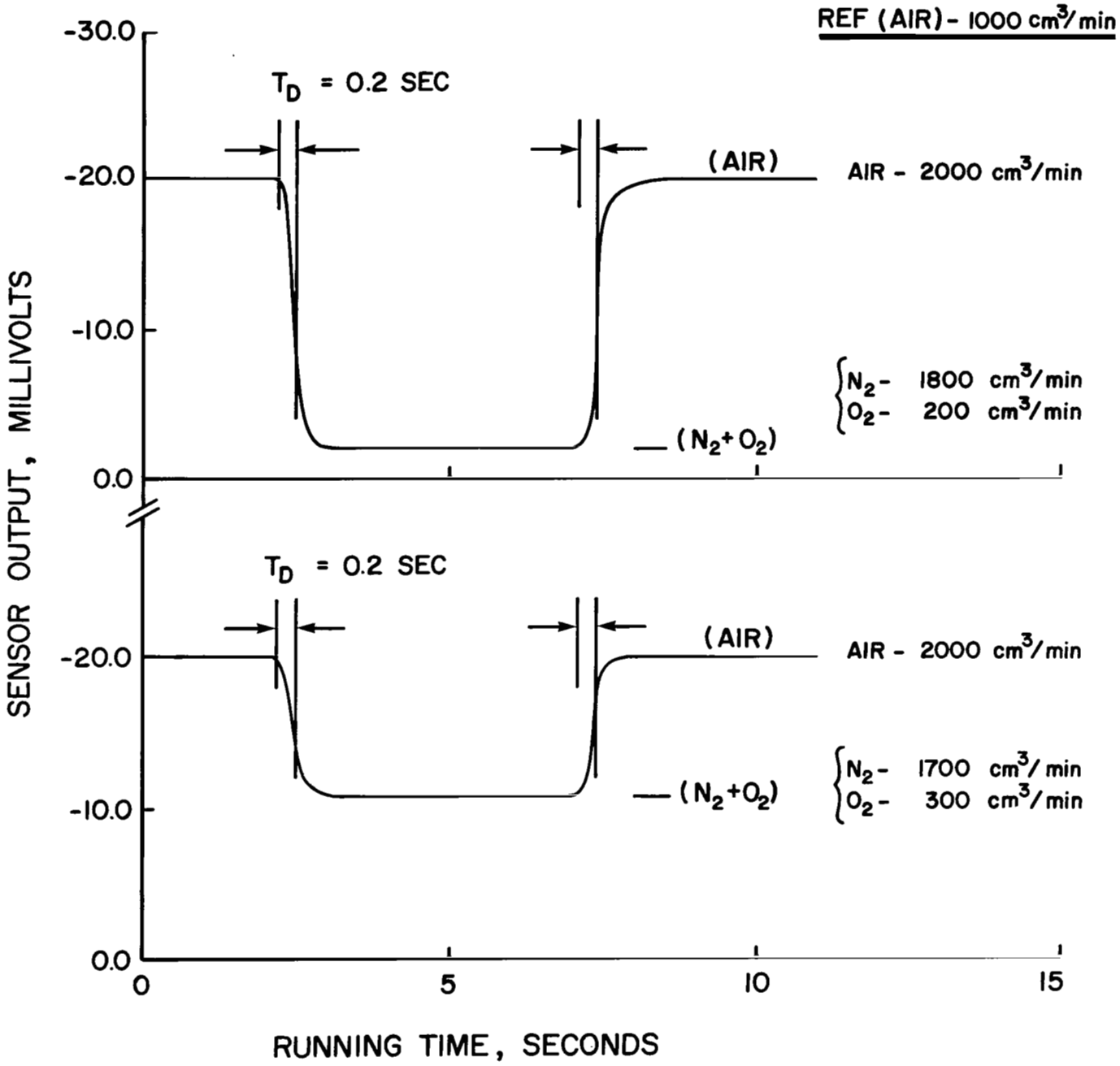

Figure 13.- Zirconium oxide sensor response time for two different $N_2 + O_2 \rightleftarrows$ air changes.

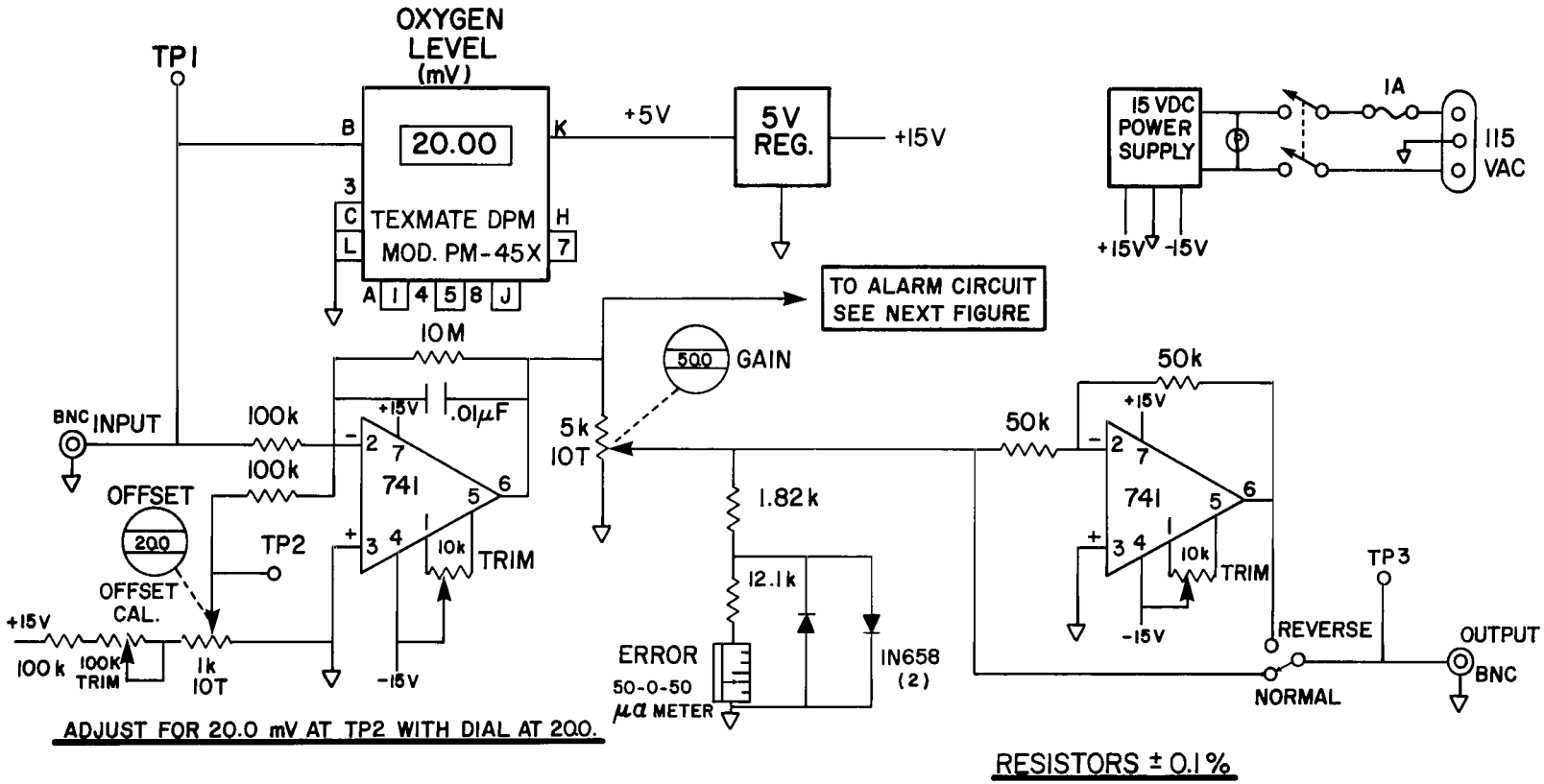

Figure 14.- Oxygen-concentration servo control circuit.

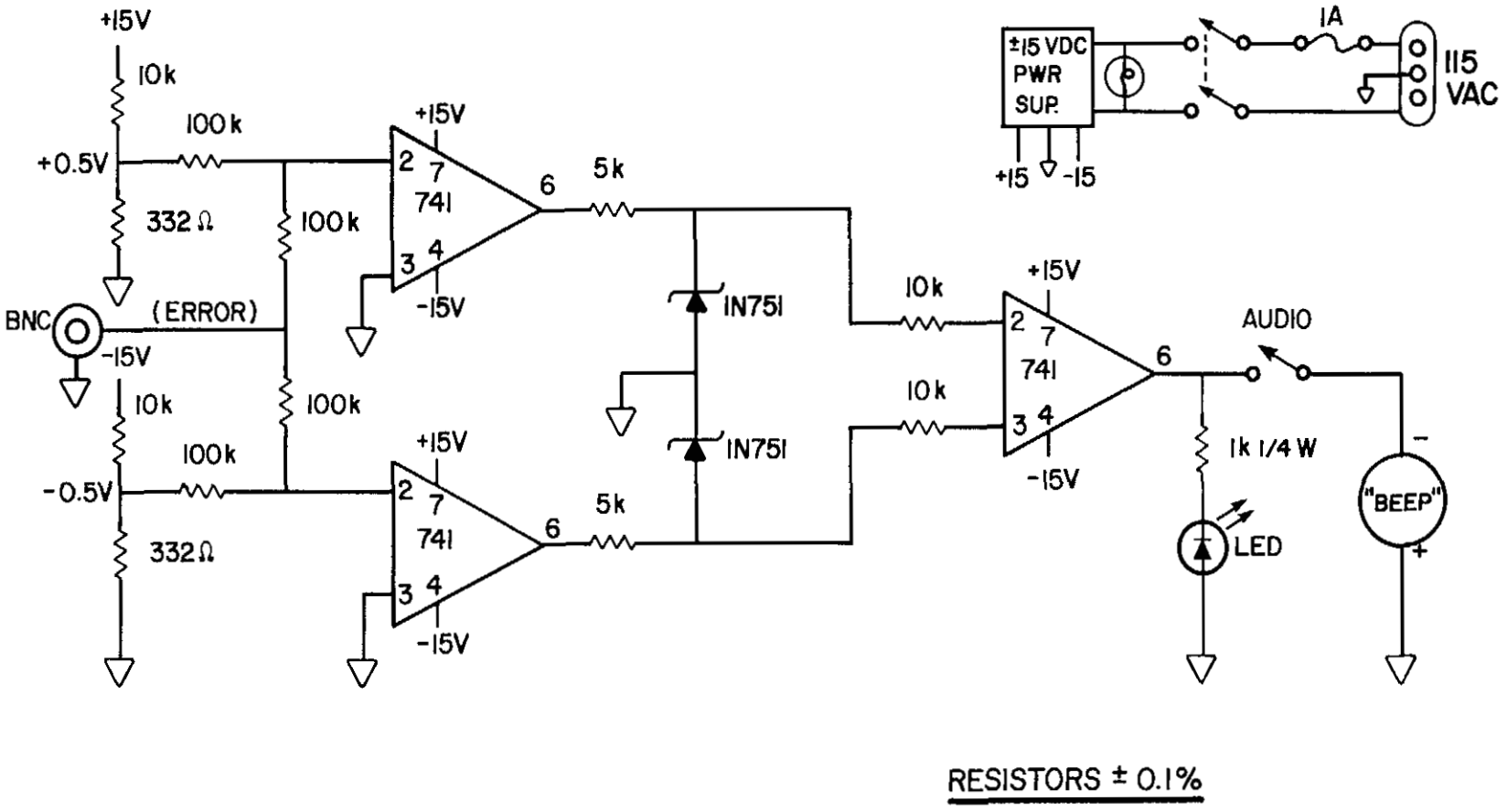

Figure 15.- Oxygen-limit alarm circuit.

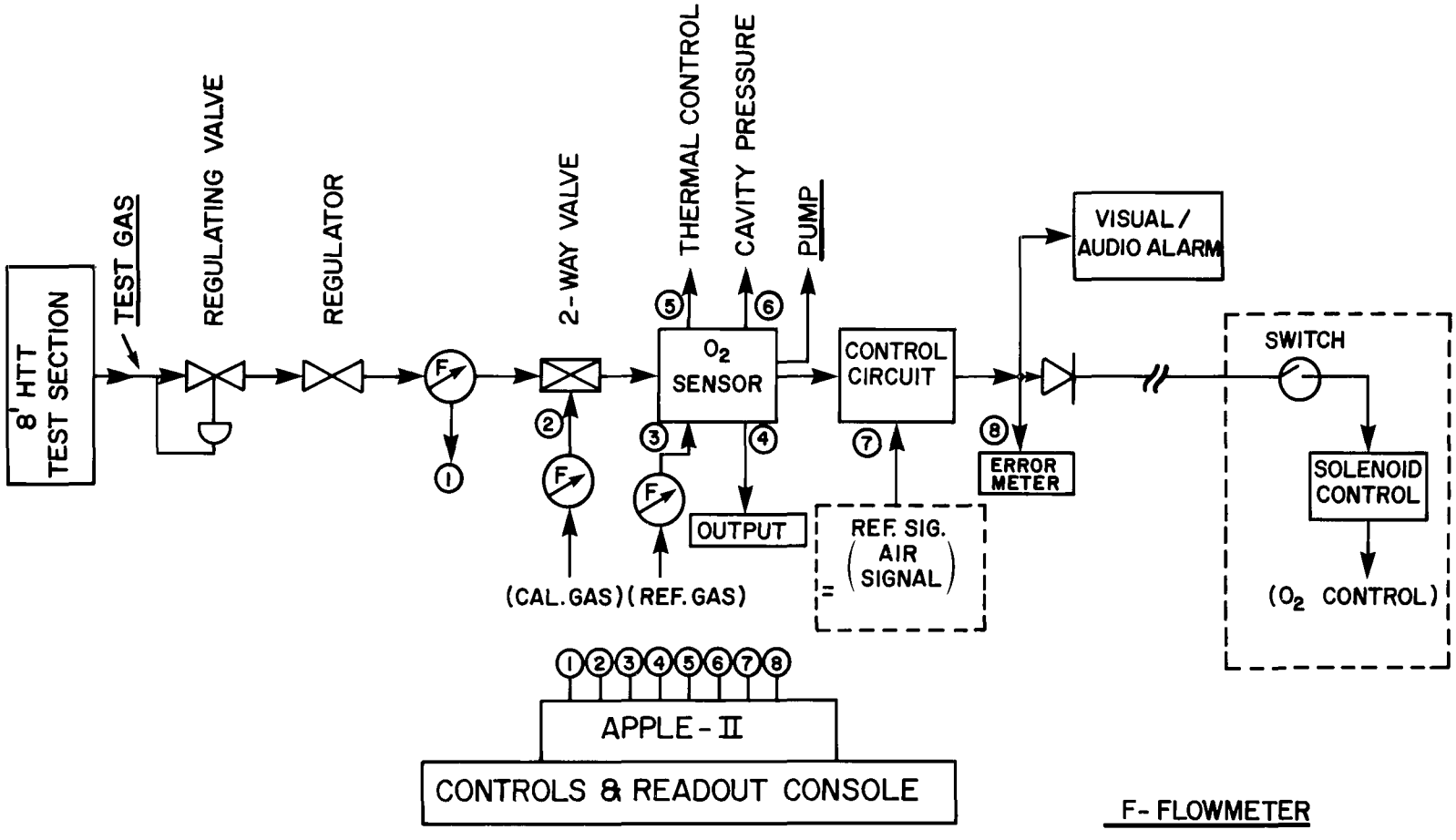

Figure 16.- Schematic diagram of the oxygen-monitoring and control system for Langley 8-Foot High-Temperature Tunnel.

1. Report No.	2. Government Accession No.	3. Recipient's Catalog No.
NASA TP-2218		

4. Title and Subtitle	5. Report Date
PROPOSED FAST-RESPONSE OXYGEN MONITORING AND CONTROL SYSTEM FOR THE LANGLEY 8-FOOT HIGH-TEMPERATURE TUNNEL	November 1983
	6. Performing Organization Code 505-33-53-14
7. Author(s) Jag J. Singh, William T. Davis, and Richard L. Puster	8. Performing Organization Report No. L-15666
9. Performing Organization Name and Address NASA Langley Research Center Hampton, VA 23665	10. Work Unit No.
	11. Contract or Grant No.
12. Sponsoring Agency Name and Address National Aeronautics and Space Administration Washington, DC 20546	13. Type of Report and Period Covered Technical Paper
	14. Sponsoring Agency Code

15. Supplementary Notes

16. Abstract

A fast-response oxygen monitoring and control system, based on a Y_2O_3-stabilized ZrO_2 sensor, has been developed and tested in the laboratory. The system is capable of maintaining oxygen concentration in the CH_4-O_2-air combustion product gases at 20.9 ± 1.0 percent. If the oxygen concentration in the exhaust stream differs from that in normal air by 25 percent or more, an alarm signal is provided for automatic tunnel shutdown. The overall prototype system response time was reduced from about 1 sec in the original configuration to about 0.2 sec. The basis of operation and the results of laboratory tests of the system are described.

17. Key Words (Suggested by Author(s))	18. Distribution Statement
Hypersonic vehicle development Methane combustion in oxygen-enriched air Oxygen monitoring Oxygen control Electrochemical cell Nernst equation Oxygen partial pressure monitor Y_2O_3-stabilized ZrO_2 sensor Fast response time	Unclassified - Unlimited Subject Category 35

19. Security Classif. (of this report)	20. Security Classif. (of this page)	21. No. of Pages	22. Price
Unclassified	Unclassified	28	A03

For sale by the National Technical Information Service, Springfield, Virginia 22161

NASA-Langley, 1983

1 1U,D, 831109 S00903DS
DEPT OF THE AIR FORCE
AF WEAPONS LABORATORY
ATTN: TECHNICAL LIBRARY (SUL)
KIRTLAND AFB NM 87117